Electronic Supplementary Material (ESI) for Journal of Materials Chemistry A.

Supporting Information

Solvent-Free Synthesis of a Porous Thiophene Polymer by Mechanochemical Oxidative Polymerization

S. Grätz,[a] M. Oltermann,[a] E. Troschke,[a] S. Paasch,[b] S. Krause,[a] E. Brunner[b] and L. Borchardt[a]

[a] Chair of Inorganic Chemistry I, Technische Universität Dresden,
Bergstraße 66, D-01069 Dresden, Germany.

[b] Chair of Bioanalytical Chemistry, Technische Universität Dresden
Bergstraße 66, D-01069 Dresden, Germany.

Table of Contents

1 General methods

Argon physisorption measurements were performed at 87 K on an Autosorb-IQ-C-XR (Quantachrome Instruments). High purity gases were used for physisorption measurements (Ar: 99.999%). Specific surface areas (SBET) were calculated using the equation from Brunauer, Emmet and Teller (BET) in a relative pressure range that fits to the consistency criteria proposed by Rouquerol and Llewellyn.[1] Pore size distributions were calculated using the Quenched Solid Density Functional Theory (QSDFT) method for carbon (slit pores, equilibrium kernel) on the adsorption branch. Total pore volumes were determined from the adsorption branch at p/p_0 = 0.95. Prior to physisorption experiments, all samples were activated at 423 K for 24 h under vacuum.

Ball mill syntheses were carried out in a Fritsch Pulverisette 7 premium line planetary ball mill operating at a rotation speed of 800 rpm. The syntheses were performed a 45 mL zircon dioxide grinding jar with 22 zircon dioxide balls (10 mm in diameter) if not stated otherwise.

Bulking material: Briefly, a bulking agent can be interpreted as an inert additive to the reaction. The size of the milling jar (45 mL in our case) requires a minimum amount of reactants in the reaction jar (ball-to-powder ratio), otherwise the milling balls will collide without transferring the energy of the collision onto the reactants, thus causing enhanced abrasion. We used an inert bulking agent - NaCl - to gain control over the reactions scale. This method was first described by Konnert et Al.[2] Since we used a total mass loading of 10 g in the milling jar for all runs, we added the amount of bulking agent that was necessary to reach 10 g. Alternatively we could have also increased the amount of $FeCl_3$ do deal with this issue.

Elemental analysis were carried out on a vario MICRO cube Elemental Analyzer by Elementar Analysatorsysteme GmbH in CHNS modus.

Infrared spectroscopy (IR) was carried out on a BRUKER Vertex 70 with a Specac Golden Gate ATR unit. A resolution of 2 cm-1 was utilized and the resulting spectra were treated with ATR-correction by the OPUS 6.5 software.

Powder X-ray diffraction (PXRD) patterns were collected in transmission geometry (MYTHEN 1K detector) with a STOE STADI P diffractometer operated at 40 kV and 30 mA with a Ge Monochromator using Cu-Kα1 radiation.

Nitrogen physisorption measurements were performed at 77 K on a Quantachrome Quadrasorb apparatus. High purity gases were used for physisorption measurements (N2: 99.999%).

Simulation of structural model for MPT-1: A model of the crystal structure of MPT-1 was established by using Material Studio 5[*]. The structure was initially modelled in a hexagonal unit cell with space group *P*3 a symmetry common in hexagonal COFs. The geometry and unit cell parameters were optimized by using the forcite module with default settings. The final unit cell parameters are 20.7305 Å and 3.5891 Å for a/b and c, respectively. Due to the low crystallinity of MPT-1 no structural refinement of the diffraction pattern could be performed further validating the proposed model.

Solid state ^{13}C CP-MAS NMR experiments were performed on a Bruker Ascend 800 spectrometer operating at 201.2 MHz for ^{13}C using a commercial double resonance 3.2 mm MAS NMR probe. Ramped ^{1}H-^{13}C cross-polarization (CP, contact time: 4 ms, pulse repetition time: 3 s) and SPINAL ^{1}H-decoupling was applied. The MAS

---

[*] Material Studio 5.0 (Accelrys Software Inc., San Diego, USA, 2009)

frequency was 15 kHz. The ^{13}C chemical shifts were referenced with adamantane. Peak assignment was done utilizing ACD Labs[†].

Scanning electron microscopy (SEM/EDX) images were obtained using a Hitachi SU8020 SEM equipped with a secondary electron (SE) detector. Prior to the measurement the samples were prepared on an adhesive carbon pad and sputtered with gold to obtain the necessary electron conductivity.

Thermogravimetric analysis (TGA) was performed on a NETZSCH STA 409 PC/PG system using alumina crucibles under argon stream with the heating rate of 10 K min-1.

2 Materials

1,3,5-Tris(2-thienyl)benzene (TCI, >98%), 1,3,5-Tris(N-carbazolyl)benzene (Aldrich, >97%), Iron(III) chloride (anhydrous; ABCR, >98%), and Sodium chloride (Güssig, >98%) were used as received.
Zirconium oxide (Type ZY-S) milling balls with a diameter of 10 mm were purchased from Sigmund Lindner GmbH. The average weight of one milling ball is 3.19 ± 0.05 g.
Zirconium oxide (Type ZY-S) milling balls with a diameter of 15 mm were purchased from Sigmund Lindner GmbH. The average weight of one milling ball is 11.4 ± 0.5 g.

3 Synthetic Procedures

In a typical mechanochemical synthesis of MTP-1, 0.3 g of 1,3,5-Tris(2-thienyl)benzene (0.925 mmol), 1.8 g iron chloride (11.1 mmol, 12 eq.) and the inert bulking material 0.9 g sodium chloride were transferred into a 45 mL grinding jar with twenty-two 10 mm-diameter grinding balls. The educts were then milled for 60 min at 400 rpm in a Fritsch Pulverisette 7 premium line planetary ball mill. After the reaction, the grinding jar was opened and the reaction mixture was poured into water. The crude product was consequently washed with water and soxleth extracted with water and THF before it was dried at 70°C. MTP-1 was obtained as a yellowish powder (290 mg, yield: 98%).

For the optimization experiments and their parameters see the next chapter.

For the synthesis of MCP-1, 0.3 g of 1,3,5-tri(9-carbazolyl)-benzene (0.521 mmol), 1.02 g iron chloride (6.25 mmol, 12 eq.) .and the inert bulking material 8.68 g sodium chloride chloride were transferred into a 45 mL grinding jar with twenty-two 10 mm-diameter grinding balls. The educts were then milled for 60 min at 400 rpm in a Fritsch Pulverisette 7 premium line planetary ball mill. After the reaction, the grinding jar was opened and the reaction mixture was poured into water. The crude product was consequently washed with water and soxleth extracted with water and THF before it was dried at 70°C. MCP-1 was obtained as a beige powder (150 mg, yield: 50%).

[†] ACD/C+H NMR Predictors and DB 2017.1.3, *Advanced Chemistry Development*, Inc., Toronto, ON, Canada, www.acdlabs.com, 2017.

4 Optimization - Design of Experiment

Design of experiments describes a methodological variation of parameters in order to get the most information out of a minimum number of experiments. The data is therefore collected and a regression function is calculated in order to fit the investigated result (e.g. yield) with the chosen parameters in order to determine their influence. Since it is a statistical approach the variance of the experiment is taken into consideration as well. This can be accomplished by repeating certain experiments. It is beneficial to repeat the centre points that are introduced into the set-up to detect non-linear behaviour because their all parameters are at under non-extreme conditions. The choice of parameters and their step size is crucial for precise results. It should be noted that it is in general better to choose them in such a matter as to obtain maximum effects, to better differentiate the effects from the normal variance. Furthermore the runs are conducted in a randomized order to spread influence from random disturbances (different batches of starting material, lab temperature, etc.) evenly over all experiments.

The impact of the synthesis parameters applied on the mechanochemical oxidative polymerization of 1,3,5-Tris(2-thienyl)benzene were studied in a factorial 2^{7-3} factorial design with a resolution of IV with a centre point that was repeated once. The parameters are varied in 2 levels, as represented in Table S4.

Table S1. 2 level, fractional DOE layout with center points, randomized order.

run order	eq. $FeCl_3$	ball/powder ratio	ball size	milling time	rpm	yield	SSA_{BET} a)
1	12,0	0,033	15	60	400	**98**	**2002**
2	12,0	0,033	10	60	400	**88**	**1989**
3	12,0	0,111	10	60	400	**96**	**1927**
4	3,0	0,033	10	60	400	**36**	**582**
5	7,5	0,072	15	35	600	**97**	**1552**
6	7,5	0,072	10	35	600	**73**	**1384**
7	3,0	0,111	15	60	400	**31**	**850**
8	3,0	0,033	15	10	400	**22**	**898**
9	3,0	0,111	15	10	800	**32**	**675**
10	12,0	0,033	15	10	800	**91**	**1092**
11	12,0	0,111	15	10	400	**72**	**1469**
12	12,0	0,111	10	10	800	**86**	**1894**
13	3,0	0,033	10	10	800	**51**	**477**
14	3,0	0,033	15	60	800	**81**	**266**
15	12,0	0,033	10	60	800	**93**	**1378**
16	7,5	0,072	15	35	600	**85**	**1227**
17	7,5	0,072	10	35	600	**85**	**1412**
18	3,0	0,111	10	10	400	**26**	**842**
19	12,0	0,111	15	60	800	**69**	**1585**
20	3,0	0,111	10	60	800	**61**	**250**

The main effect plots for SSA and yield of the reaction are given in Figure S1 and S2. The main effect plots can give one an idea of the influence of a single parameter and helps to visualize the results from Table S1. In both cases the main influence seems to be the equivalents of $FeCl_3$. In addition a negative influence of the milling speed can be observed for the SSA. The observations are also verified by the Pareto plots (Figure S3 and S4) which only point out said parameters as significant.

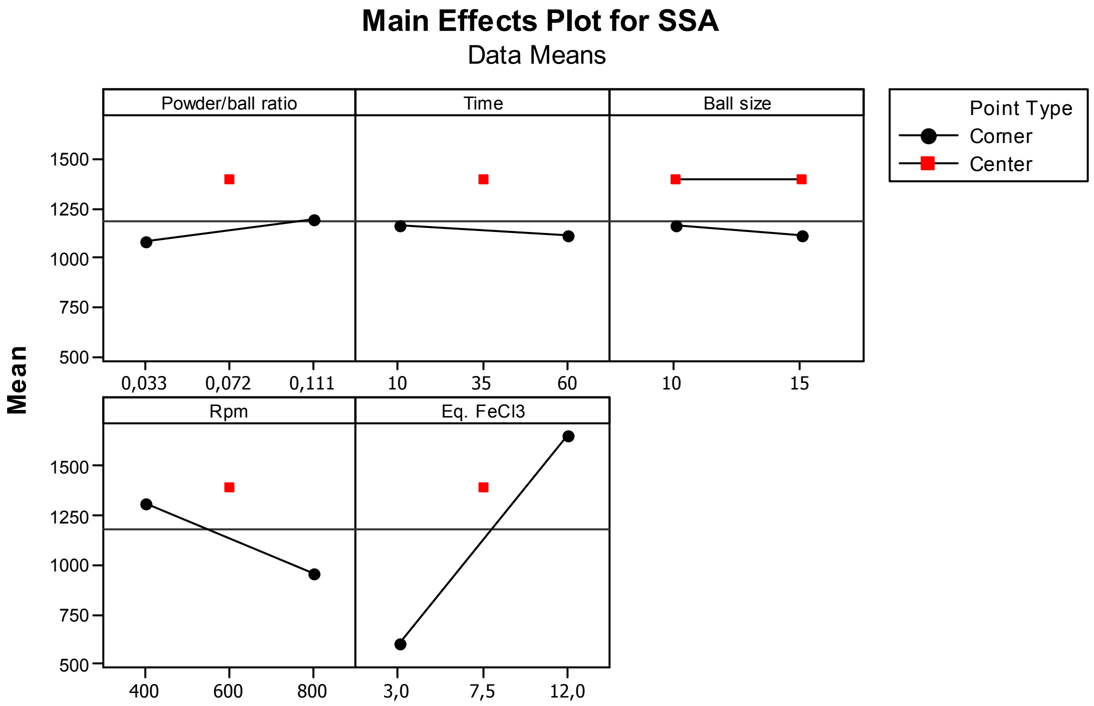

Fig. S1. Results of the DOE (cf. TableS1). Visualization of the main effects on the surface area of the MPT polymer as presented in the Pareto chart. Red dots represent the center point experiments with an average value of each of the parameters.

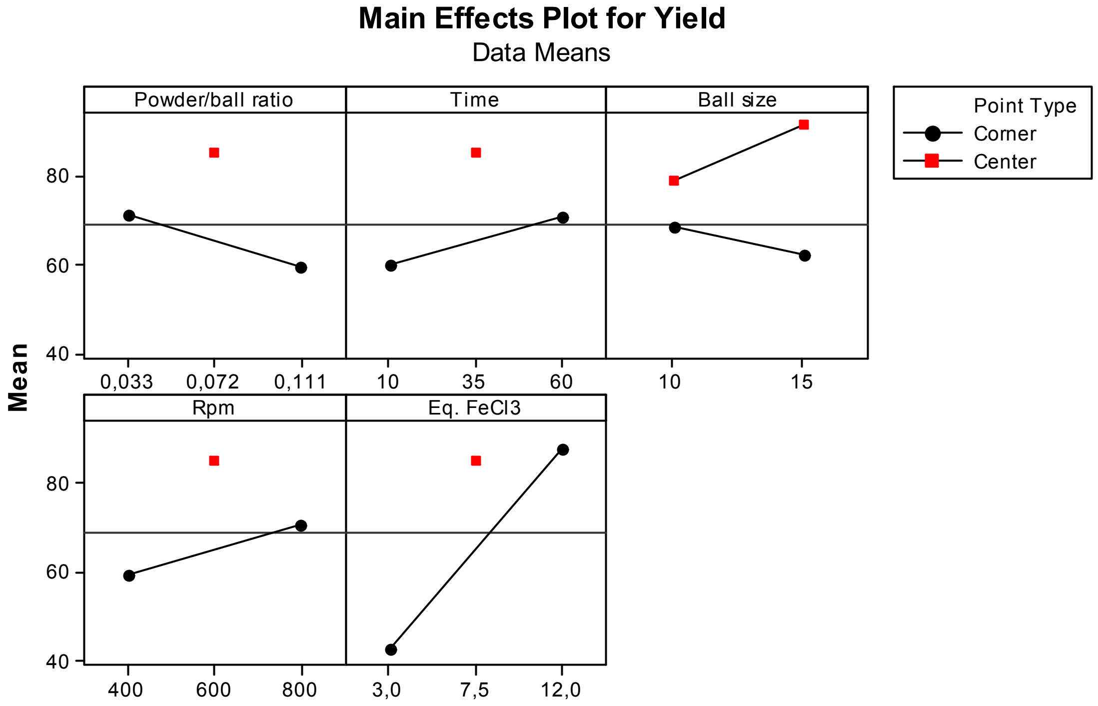

Fig. S2. Results of the DOE (cf. TableS1). Visualization of the main effects on the yield of the MPT polymer as presented in the Pareto chart. Red dots represent the center point experiments with an average value of each of the parameters.

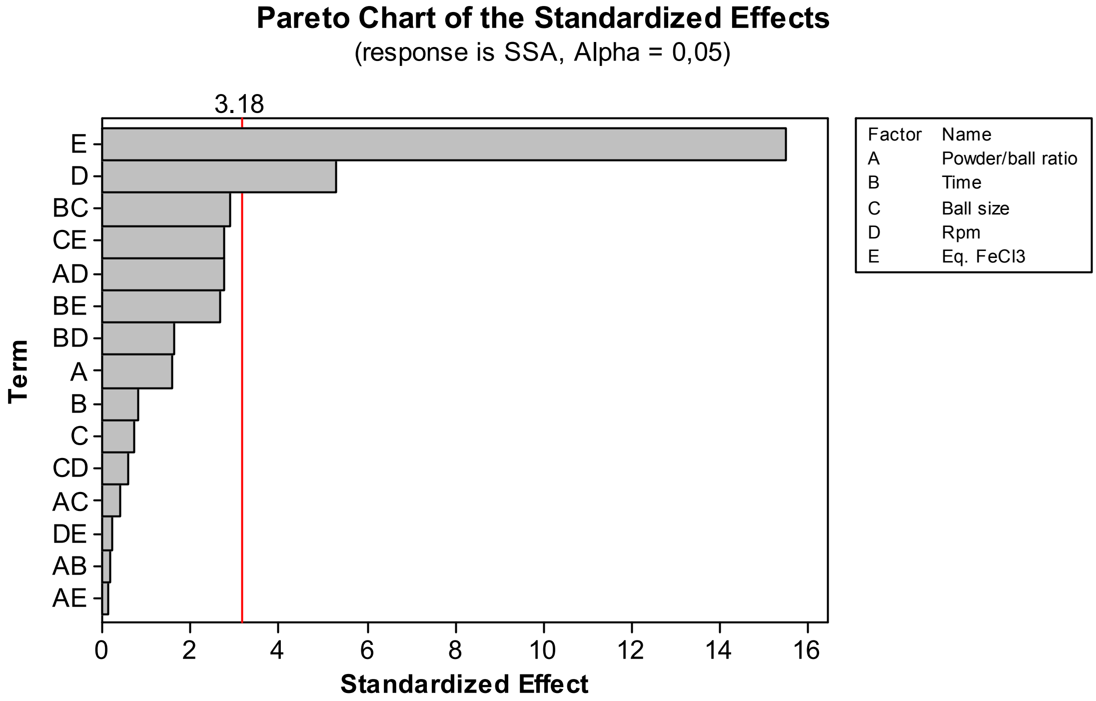

Fig. S3. Results of the DOE (cf. TableS1). The Pareto chart shows a significant influence of factor E (Eq. $FeCl_3$) and D (Ball size) on the surface are of the MTP polymer.

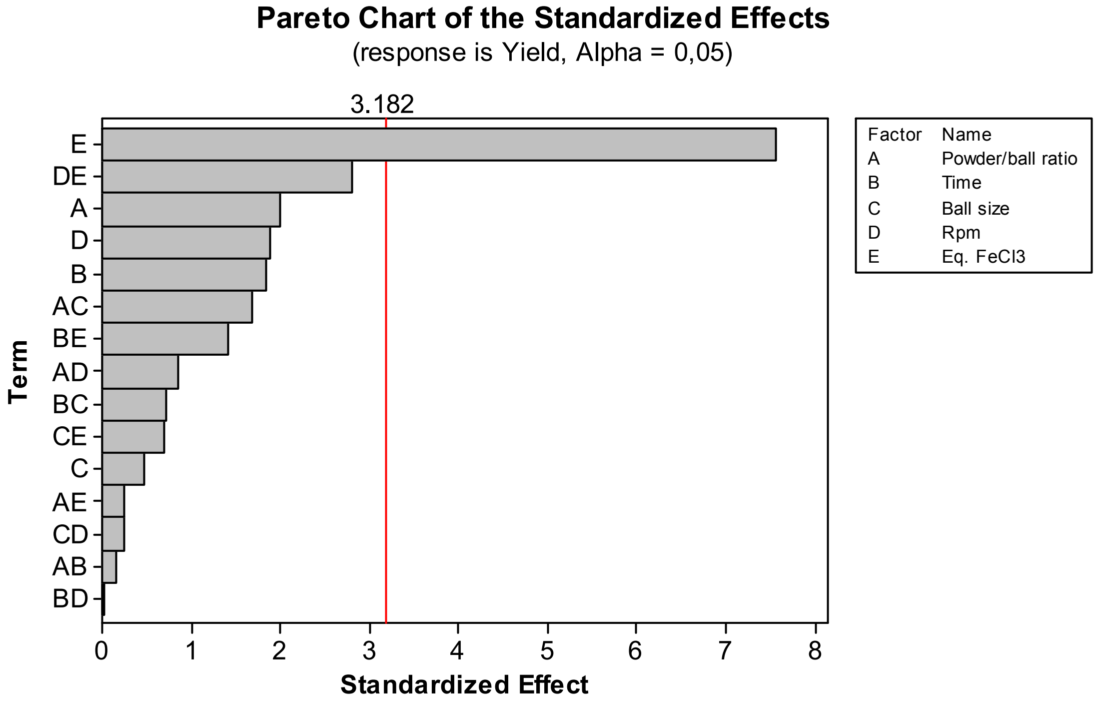

Fig. S4. Results of the DOE (cf. TableS1). The Pareto chart shows a significant influence of factor E (Eq. $FeCl_3$) on the yield are of the MTP polymer.

5 Characterization

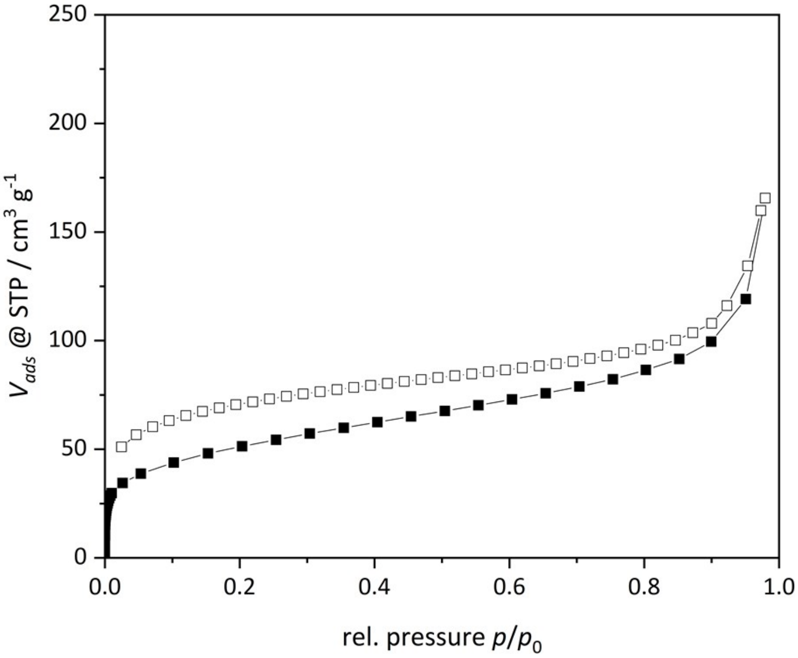

Fig. S5. Low pressure argon physisorption isotherm of the solution based reference MPT-1-ref, exhibiting a way lower surface area than the mechanochemical procedure and showing the typical swelling behavior.

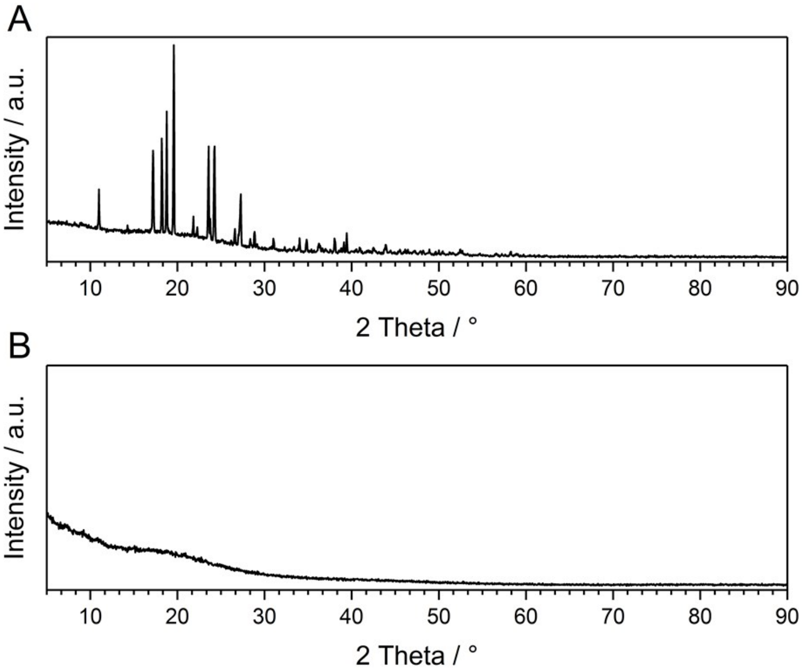

Fig. S6. X-ray diffraction pattern of A: 1,3,5-Tris(2-thienyl)benzene B: MPT-1 highlighting the amorphous structure of the polymer.

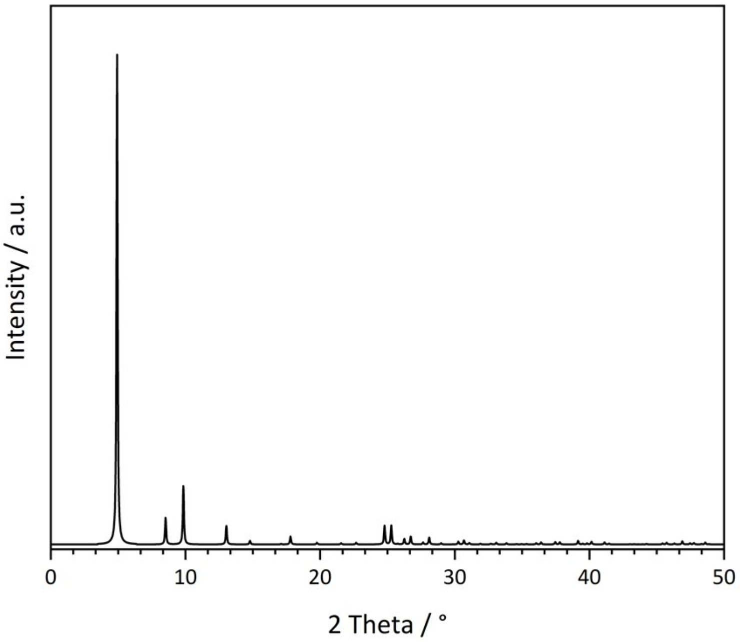

Fig. S7. Simulated powder X-ray diffraction pattern of MPT-1.

Table S2. Elemental analysis.

Sample	Found (%)				Calculated (%)			
	C	H	N	S	C	H	N	S
MPT-1	60.37	2.027	-	26.745	67.25	2.82	-	29.92
Refernece[3]	62.41	2.42	-	26.43				

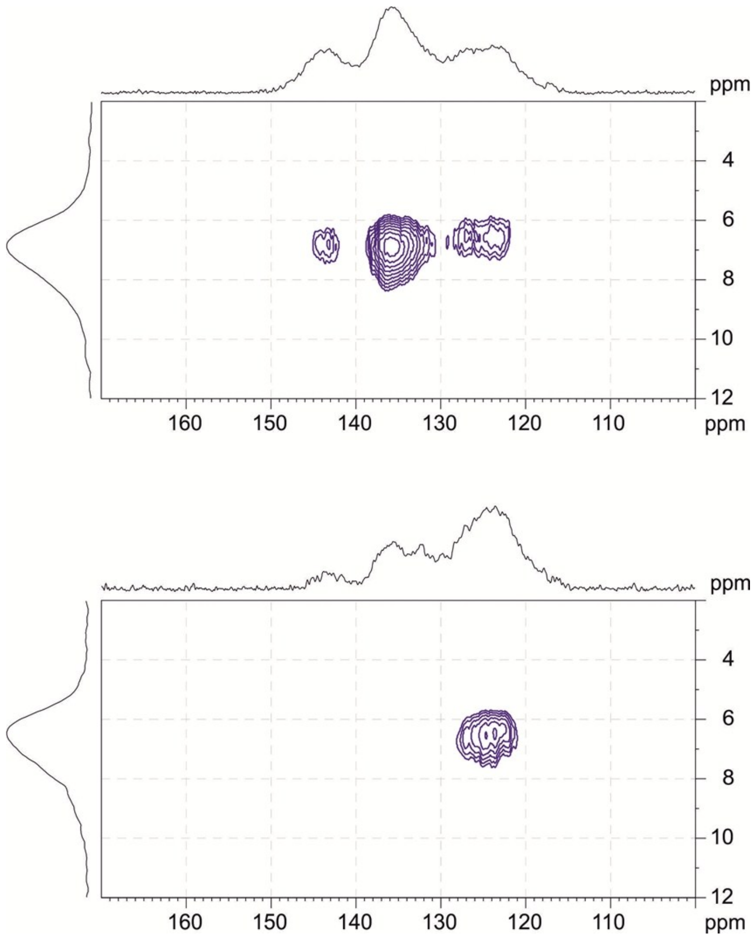

Fig. S8. ^{1}H-^{13}C HETCOR NMR spectra of MTP-1 at contact times of 4 ms (Top) and 0.7 ms (Bottom). These experiments confirm the peak assignment for MTP-1 provided in Fig.3. At the long contact time (4 ms), correlations between all carbon atoms and protons (quaternary C´s and CH groups) appear whereas at a short contact time of 0.7 ms, only CH groups show up in the spectrum.

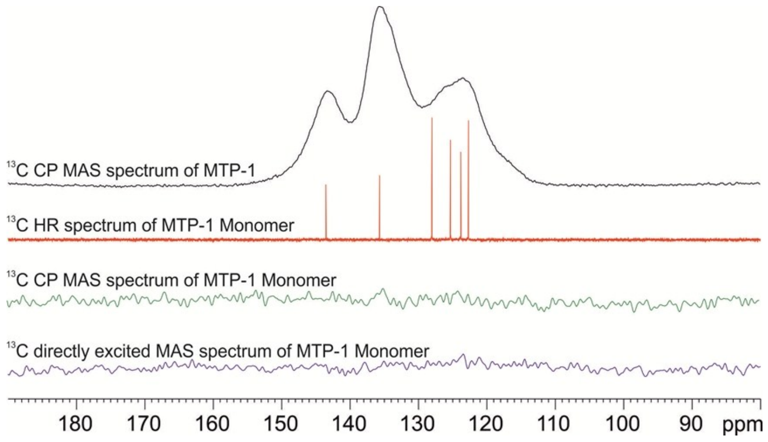

Fig. S9. Comparison of the ^{13}C CP MAS NMR spectrum of MTP-1 (black) with the ^{13}C NMR spectra of the MTP-1 monomer. The red spectrum is the ^{13}C High-Resolution (HR, liquid state) NMR spectrum measured for MTP-1 monomer dissolved in $CDCl_3$. The solid-state NMR spectra (green, blue) of the monomer only show extremely broad lines for both, ^{1}H-^{13}C cross polarization (CP) and direct excitation. This can be explained by disorder of the solid-state of the monomer. Both, static and dynamic disorder (thermal mobility) can in principle contribute to this extreme line broadening.

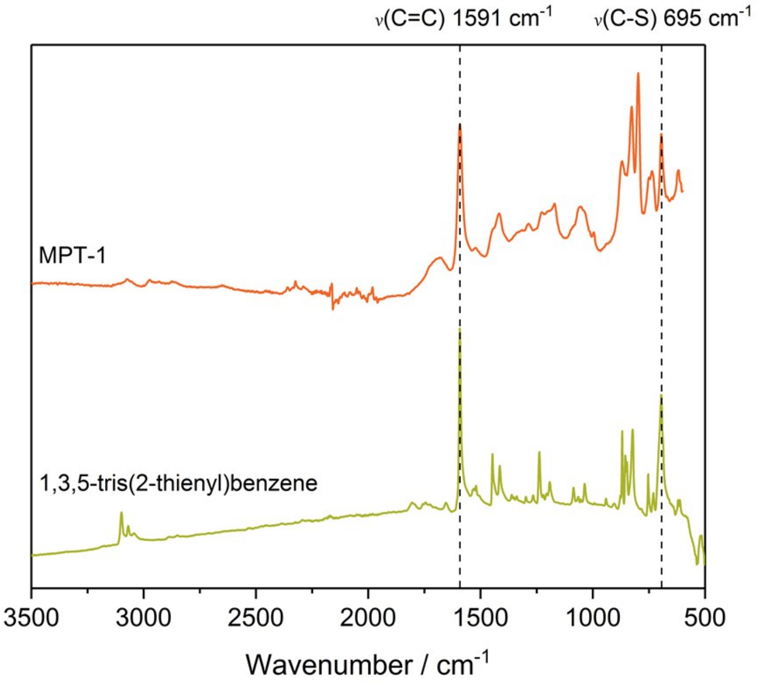

Fig. S10. FT-IR spectra of MPT-1 and the monomer 1,3,5-tris(2-thienyl)benzene showing intact C-S vibrations for the polymer.

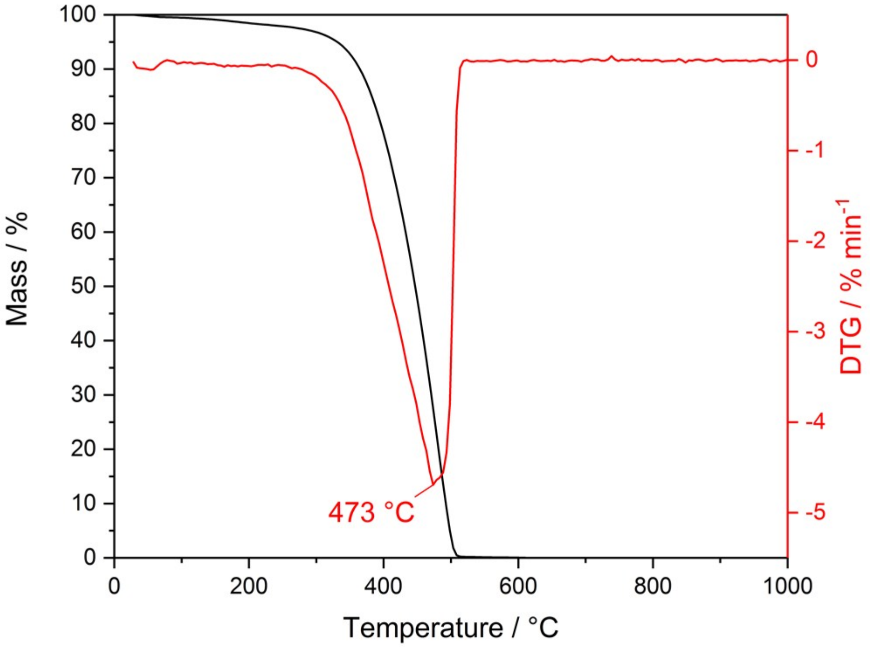

Fig. S11. TGA curve of MTP-1 under air showing one major degradation step with a peak at 473 °C as visible by the DTG plot. The complete degradation also hints towards no contamination with either the oxidant or milling material.

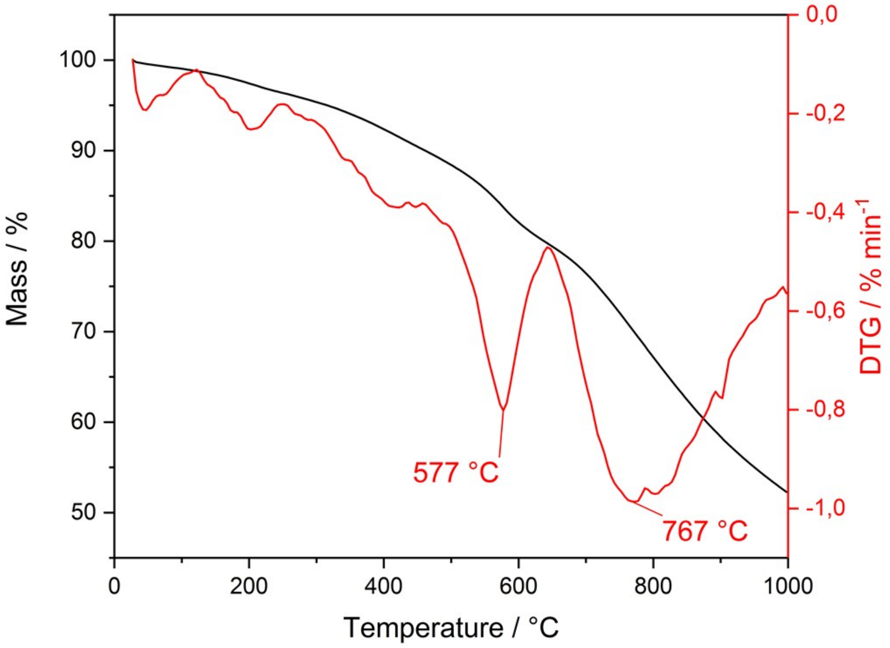

Fig. S12. TGA curve of MTP-1 under argon showing several smaller degradations step as visible by the DTG plot.

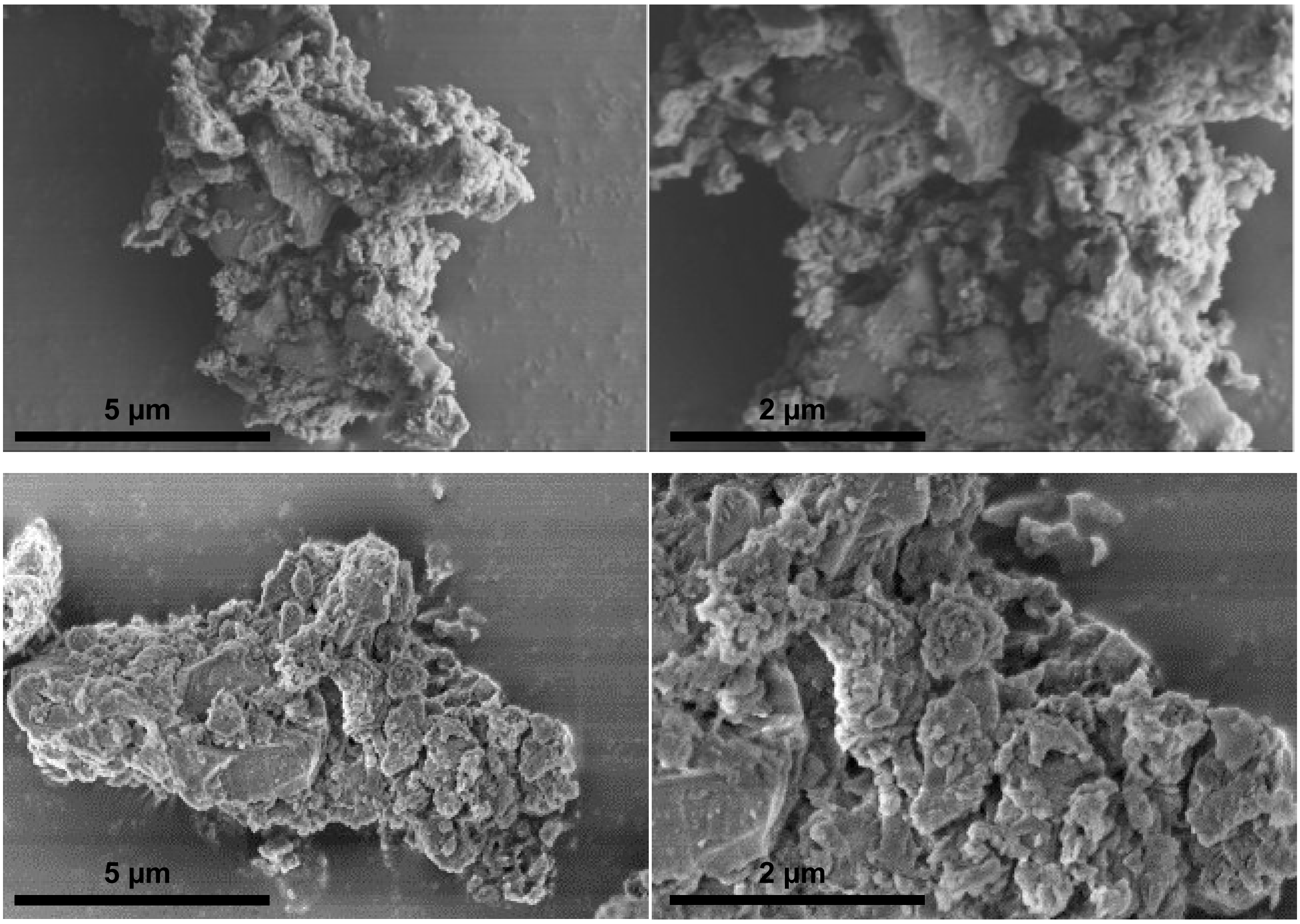

Fig. S13. SEM images of two different particles and magnifications of MPT-1. Larger flakes are agglomerated with smaller unevenly shaped particles to form big agglomerates.

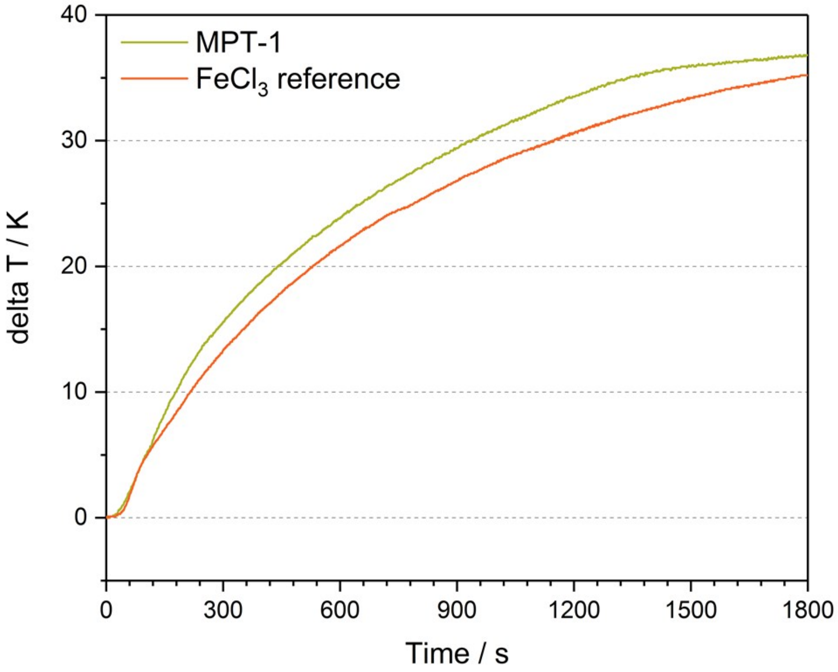

Fig. S14. Development of the relative vessel temperature during the milling process comparison of MPT with a vessel filled with $FeCl_3$ as reference at 800 rpm.

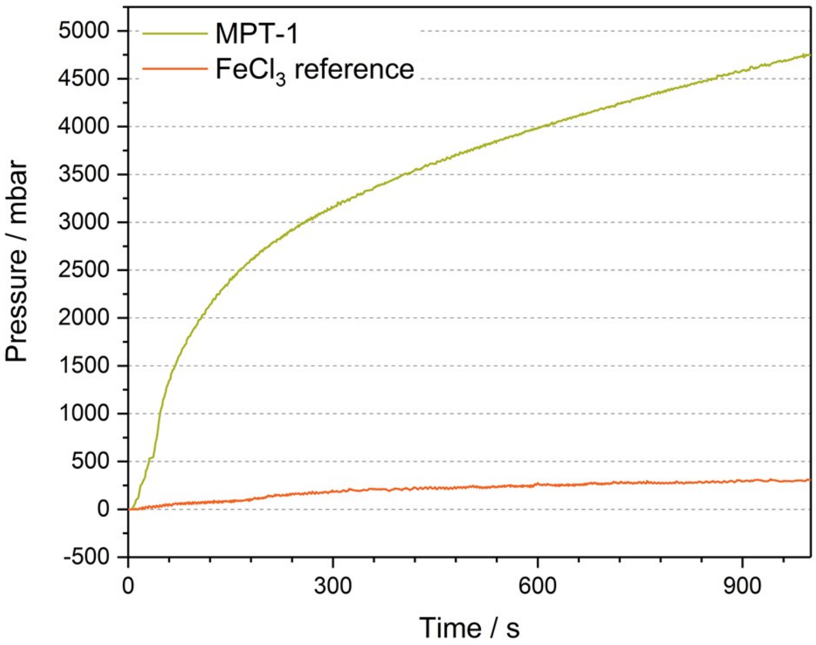

Fig. S15. Development of the relative vessel pressure during the milling process comparison of MPT with a vessel filled with $FeCl_3$ as reference at 800 rpm. After the first steep increase (~300s) it transitions into a smaller sloped ascend due to the rise in vessel temperature.

6 MCP-1 Discussion

While Dai and co-workers briefly investigated the influence of the milling parameters and their optimized conditions lead to a polymer with a surface area of 940 m^2g^{-1}, while our protocol produces a polymer with 1710 m^2g^{-1} (Table 1, Fig. S16) - almost twice as high. The differences between the two procedures are not only in the eq. of $FeCl_3$ but also the fact, that a mixer ball mill was used for the latter. The transfer of protocols between these two mill types bears many challenges. While a direct comparison of these two methods for the production of porous polymers would be of interest, such a study does not exist to the best of our knowledge.

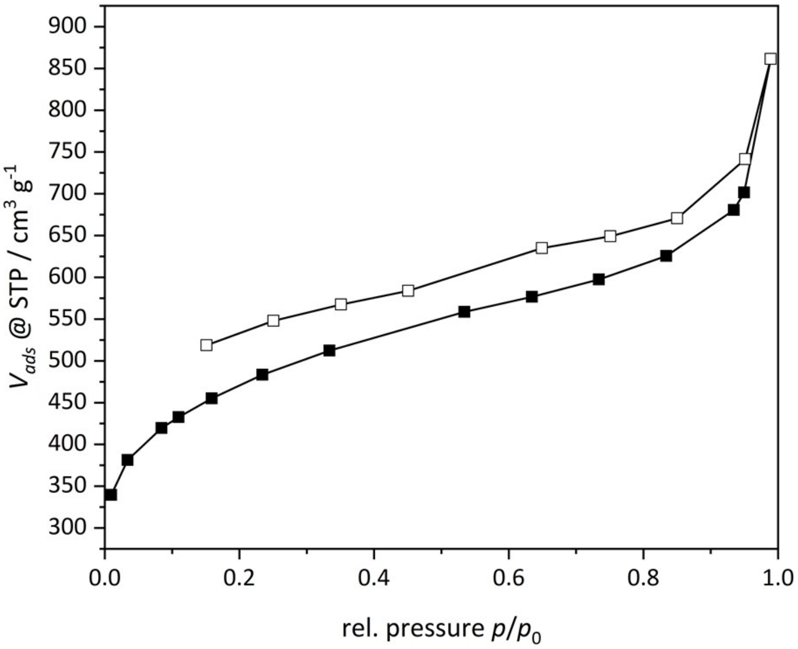

Fig. S16. Argon physisorption isotherm of MCP-1 obtained from 1,3,5-tri(9-carbazolyl)-benzene

7 References

1 J. Rouquerol, P. Llewellyn and F. Rouquerol, in *Studies in Surface Science and Catalysis*, Elsevier, 2007, vol. Volume 160, pp. 49–56.
2 L. Konnert, A. Gauliard, F. Lamaty, J. Martinez and E. Colacino, *ACS Sustain. Chem. Eng.*, 2013, **1**, 1186–1191.
3 J. Schmidt, J. Weber, J. D. Epping, M. Antonietti and A. Thomas, *Adv. Mater.*, 2009, **21**, 702–705.

8 Author contributions

Sven Grätz	Preparation of the manuscript, planning of the experiments, GTM measurements, XRD measurements
Maike Oltermann	Synthesis and characterization of MPT-1, IR-measurements
Erik Troschke	Planning of the experiments, Proof-of-Principle experiments
Simon Krause	Simulation of the structure, simulation of PXRD pattern
Silvia Paasch	Measurement and interpretation of ^{13}C CP-MAS NMR
Eike Brunner	Supervision of ^{13}C CP-MAS NMR
Lars Borchardt	Project coordination and supervision